# Shape functions for a triangle with a side node: A Formulation in the physical domain

Gautam Dasgupta
Civil Engineering and Engineering Mechanics
Columbia University, New York, NY 10027
gd18@columbia.edu

**Abstract**

During the seventies, in a monograph Wachspress established a consistent way to evaluate shape functions for polygonal finite elements and their three-dimensional counterparts. In the physical $x - y - z$ coordinates, using projective geometry concepts, he derived interpolants in the form of ratios of polynomials. Therein, he also demonstrated that square root expressions were needed to account for singularities like concavities. The author transformed shape functions for the popular four-node isoparametric formulation from $\eta - \xi$ computational square into the physical $x - y$ domain and demonstrated the presence of square root terms in $x - y$ variables when no two sides were parallel. In the Padé form, by following a direct algebraic formulation, the discontinuity in shape functions due to a side node is captured in this paper using square root expressions. Within the element, the constant and linear fields are exactly represented by solving for shape functions associated with the vertices of the triangular element. Consequently, arbitrary constant strain fields, which are necessary for the *patch test*, are guaranteed unconditionally. Finally, this paper furnishes the closed form shape functions that can be easily translated into `C` and `C++` codes.

**Contents**

**List of Figures**

## 1. Introduction

Advanced applications of the finite element method in nano and bio technologies, *vide* Hornyak et al. (2008); Mow and Huiskes (2005), demand high accuracy formulations with the best approximations to expressing the basis functions. This need has rekindled interests on the Wachspress (1975) formulations in constructing finite element shape functions in the physical $x-y-z$ coordinate system. These basis functions (with local supports) are also termed as test functions and interpolants in the finite element literature.

Researchers demonstrated, *vide* Sukumar and Malsch (2006), considerable progress in improving shape functions compared to the isoparametric formulation of Taig (1961), which should be regarded to be one of the most ingenious steps in the finite element technology. Taig introduced a mapping from a unit square, in the $\eta-\xi$ computational domain for describing convex quadrilaterals where the physical coordinates $x, y$ are also interpolated from the nodal values. The same bi-linear parameterization was employed in terms of $\eta-\xi$ variables for functions and coordinates, hence the name isoparametric. Due to the Cartesian product structure of the computational domain the three-dimensional (or in any analogous higher dimension where an elliptic boundary value problem problem of mathematical physics is to be solved within a convex region) isoparametric counterparts can be easily constructed. In the interest of this paper, the focus is on two-dimensional analysis with $x-y$ and $\eta-\xi$ idealization rather than the generalization in $\Re^n$. The four node triangles and polygons with interior nodes, *vide* Shontz and Vavasis (2010); Malsch et al. (2005), have been employed in computer graphics applications quite substantially and in some specific cases for high accuracy stress analysis. These problems are close to the one that is addressed here, however, the use of the 'bubble function,' *vide* Ho and Yeh (2006), is quite different from the branch cut employed here via the square root operator.

Recent applications in computer graphics have been enriched by employing finite element shape functions as generalized splines, *vide* Sukumar (2007); Mousavi et al. (2010). These formulations have blurred the boundaries between geometric modeling and the branch of finite element that focuses on basis functions. Barycentric coordinates introduced by Möbius in 1827, which are indeed homogeneous coordinates, *vide* Yiu (2000), encompass such classes of interpolants. In CAD applications spline-based solids and surfaces, which are constructed according to the formulation introduced by Hermite (1877), can be rendered very quickly when the equations are available in the physical $x - y$ coordinates, *vide* Bernstein (1913). This is an advantage compared to isoparametric-based interpolants since transformations to and form computational domains are circumvented, *vide* Foley et al. (1996), de Boor (1978).

Triangular elements are important for a number of basic reasons starting with the Courant (1943) paper that laid the foundation of the finite element method. This has widely been recognized to be the framework for the finite element development with piecewise linear fields. From the projective geometry point of view, *vide* Coxeter (2000), the triangular element contains all characteristics of a convex polygon. Thus any embellishment to introduce a side node in a triangle should also pave the way to compute the shape functions for a polygonal element with a side node when the Wachspress formulation is employed (a short explanation of this is included in the conclusion of this paper).

Procedural programming environments, e.g. `Fortran` and in some cases `C`, are predominantly used in finite element formulations. Now the wide availability of symbolic computer mathematics programs, especially those with the functional programming capabilities, permit easy formulations of many 'almost intractable problems.' In this paper *Mathematica* is extensively used to developing the concepts and constructing algebraic expressions including their graphical displays. These symbolic algebraic expressions can be readily converted into `C` and `C`$^{++}$ codes using *MathModelica*, Fritzson (2004), and can be integrated into an engineering modeling environment with *OpenModelica*, Fritzson (2011).

### *1.1. Difficulties with modeling slope discontinuity on an edge*

Based on the Ritz (1908) formulation, piecewise functions should have $n-$ order continuity for $2n-$ order of ordinary and partial differential equations. Following Courant's ideas local test functions are then constructed for approximating solutions of elliptic partial differential equations according to the weak energy-norm. Of course, global functions to improve accuracy of solutions can also be employed following Mote (1971). Historically, the overwhelming number of the finite element basis functions have been polynomial expressions in coordinate variables, even though the Ritz formulation does not impose any such restrictions.

In order to capture the discontinuity in the slope, *vide* Figure 1, associated with the interpolant pertaining to a node that lies on a boundary edge the use of square root expressions

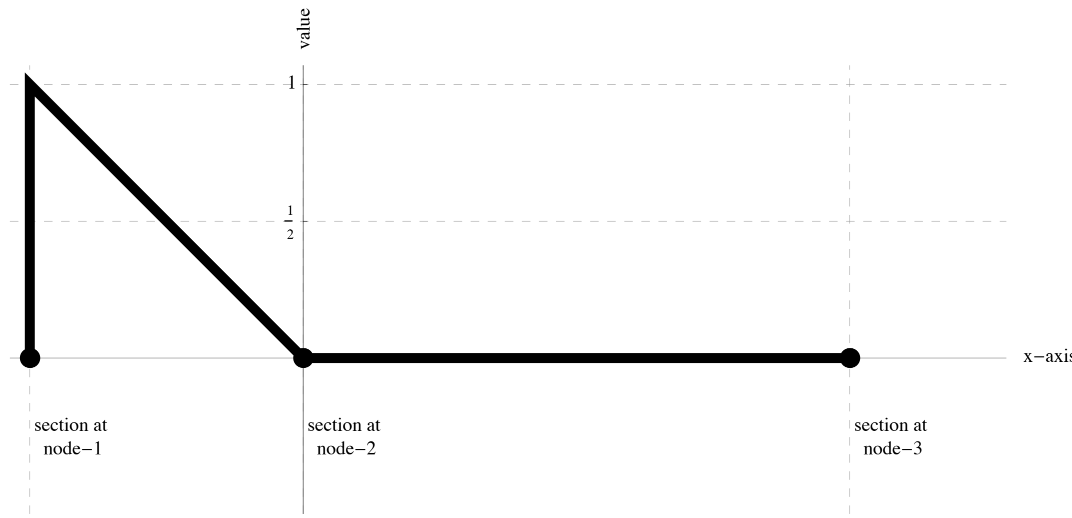


Figure 1: A bar element with end nodes 1 and 3, and intermediate node 2

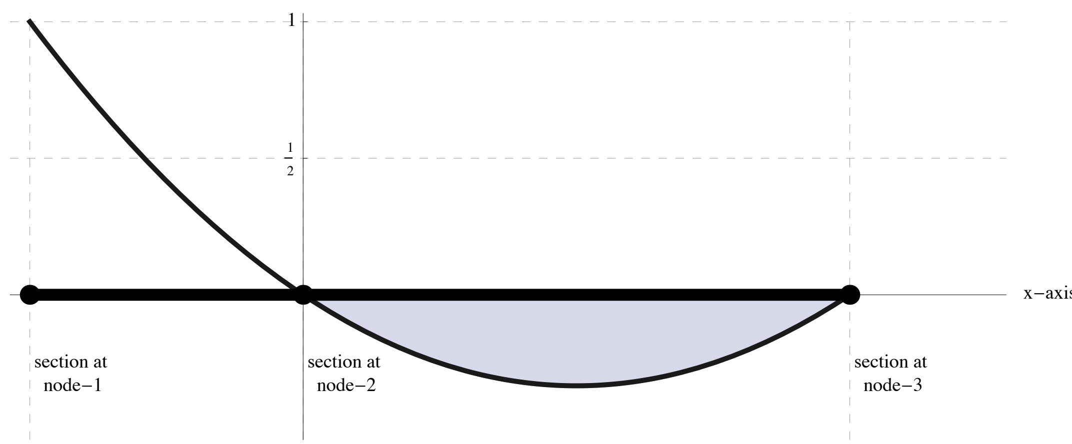


Figure 2: Polynomial shape function for node-1 — negative region is shaded

within the numerator and denominator functions is elaborated in this paper.

The inadequacy of a polynomial basis function warrants a closer look within the context of yielding approximate solutions for problems of mathematical physics. Consider a bar element in Figure 1. To solve approximately a second order differential equation, linear interpolants should be adequate according to the pioneering work of Ritz (1908). Thus for the shape function associated with node-1, one encounters the 'non-smooth' test function that cannot be reproduced by any polynomial in the $x-$variable. This is due to the fact that the support of this test function is the line segment between nodes 1 and 2. Even an Lagrangian interpolant, shown in Figure 2, is unacceptable to model elliptic partial differential equations since such a test function fails to comply with the 'maximum/minimum' theorem. To illustrate the consequences the thermo-elastic deformation in a bar can be considered with the particular focus on a finite element model for temperature distributions. Since the polynomial interpolant does not satisfy the Chebyshev (positivity) condition, the negative values between nodes 2 and 3 could yield a negative absolute temperature as the numerical result, which is by all means unacceptable from the point of view of physics. The singularity introduced by the branch cut of the square root expression circumvents this difficulty and faithfully captures the slope discontinuity shown in Figure 1.

## 2. Tessellation and basis functions in the physical $(x - y)$ domain

Needless to state that integration of the energy density function in the physical $x-y$ domain, to a large extent, hindered the popularity of the Wachspress basis functions for the last fifty years or so. This problem with integration has been solved in Dasgupta (2003a). The Wachspress formulation becomes essential in developing shape functions for finite elements with side nodes. In the interest of keeping the focus on augmenting the rational polynomial interpolants with 'square-root' expressions, the issue of exact integration to generate the stiffness matrices, *vide* Dasgupta (2008b), is not addressed here.

The following problem motivated the present formulation. In solving plane strain elasto-plastic deformations, a convex quadrilateral element was continuously compressed. This demonstration problem is illustrated in Figure 3.

A pair of horizontal (equal and opposite) compressive forces were applied along the $x-$ direction. Zero force was prescribed at the other two nodes. The area of the element was kept constant complying with the isochoric deformation constraint. Till the deformed element became a triangle, convexity was maintained and the shape function calculation was straightforward, *vide* Dasgupta (2003b). Figure 3 shows the successive deformed shapes as the node, where the compressive force is applied, translates on the x-axis towards the origin. The deformations are schematically represented with outlines. The limiting triangular shape is shown as the solid element with the shaded region.

It is desirable that the same high accuracy as in the Wachspress' formulation be maintained

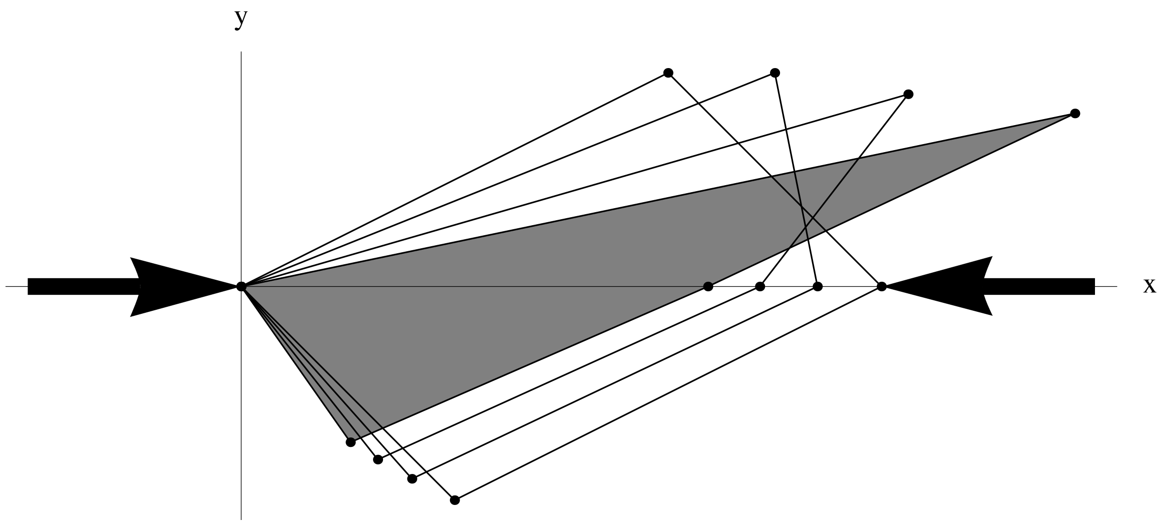


Figure 3: Elasto-plastic deformation due to Compression along x

through out. But in such a rational polynomial form for a shape function $s(x, y)$:

$$s(x, y) = \frac{\mu(x, y)}{\nu(x, y)} \tag{1}$$

the adjoint (denominator polynomial) $\nu(x, y)$ cannot be obtained for the triangular element with a side node according to the projective geometry formulation, because the strict convexity requirement is not met at the side node. The general case is shown in Figure 4.

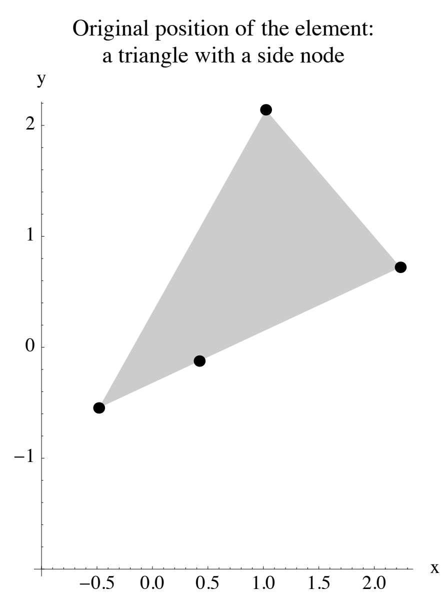


Figure 4: Original orientation

In the formulation presented in this paper, first the shape function associated with the side node is constructed as a ratio of two functions that contain square root terms. Subsequently, the three remaining shape functions are obtained as linear transformations on it. The key step of such transformations guarantees exact interpolation of arbitrary linear functions in $x - y$.

### 2.1. Conventional isoparametric basis functions in the $(\eta - \xi)$ computational frame

The isoparametric formulation for quadrilateral finite elements is applicable for triangular elements with a side node Dasgupta (2008a,b). In the isoparametric computational domain, where the $\eta - \xi$ coordinate system describe the canonical unit square, the shape functions are strictly bilinear. However, when those shape functions are transformed into the physical $x - y$ coordinate system the expressions contain square root terms. This observation provides a conceptual link to connect the intuitive isoparametric scheme with the Wachspress irrational shape functions, *vide* Wachspress (1971); Dasgupta (2008a). Furthermore, these radical subexpressions indicate that there cannot be a clear designation about the algebraic degree of interpolants since a Taylor expansion will contain all higher power $x$ and $y$ terms. However, combinations of linear terms and square roots of quadratics indicate a consistency of having the same dimensionality that is amenable to first order representation.

The isoparametric formulation by Taig is brilliant, extremely versatile and undoubtedly the most popular method to handle elements with arbitrary shapes. However, there is no geometrical foundation for this intuitive conjecture that justifies the adequacy to interpolating functions and coordinates with the same set of basis functions.

### 2.2. Computer Mathematics tools related to rational polynomials

Since the shape functions produced in this paper are meant to be employed in high accuracy finite element computations, it is important to recognize the richness of the rational form of approximations depicted in equation (1).

It was in Wachspress (1971) we found for the first time the projective geometry, Coxeter (2000), ideas in formulating finite element shape functions. The rational polynomial interpolants in the form of equation (1) resulted from the projective geometry construction of the adjoint (the denominator polynomial). Those interpolants, which have been widely applied in many branches of Physics, are known as Padé approximants, Baker and Graves-Morris (1981), named after Henri Padé (1863 – 1953) who arranged the approximants, each of which was expressed in its lowest term, into a table. Symbolic computational tools, which express an arbitrary function $f(x)$ in the form of equation (1):

$$f(x) = \frac{\mu_m(x)}{\nu_n(x)}; \quad \mu_m \text{ and } \nu_n: \text{ polynomials of degrees } m \text{ and } n, \text{ respectively} \tag{2}$$

employ the Padé table. In general, a Padé rational polynomial representation corresponds to the best approximation of a function to capture the asymptotic behaviors simultaneously near zero and infinity. For this reason, the Padé form converges when the corresponding Taylor expansion may diverge.

For a given $f(x)$ the *Mathematica* built-in function `PadeApproximant` can generate the numerator and denominator polynomials in the form of equation (2).

## 3. Formulation for shape functions: *'in a four node element only one shape function is independent'*

In displacement based formulations, the finite element shape functions are assumed to be linear along the boundary sides. In addition, for linear elasticity problems, uniform stress and strain fields are required to be reproduced exactly. This notion is germane to the *patch test,* Irons and Razzaque (1972) that ensures convergence. Within the kinematic context, it is equivalent to demanding that any arbitrary linear field be exactly represented by the shape functions. This observation leads to a useful result: "in any four node plane finite element only one shape function is independent." The remaining three shape functions can be subsequently solved, provided the corresponding nodes are not colinear, in terms of the independent shape function. We can utilize three equations, i.e., summation of all shape functions to be unity and the two that enforce the requirement of the exact reproduction of *linear* functions of $x$ and $y$, in the $x-y$ frame.

Let the four nodal coordinates for the four node plane element, shown in Figure 4, be symbolically denoted by, $\alpha$, which is given by:

$$\alpha = \{\{x_1, y_1\}, \{x_2, y_2\}, \{x_3, y_3\}, \{x_4, y_4\}\} \tag{3}$$

In order to be consistent with the designation of lists and list operations, elements of a list will be encased within curly braces, $\{\ldots\}$. Let us collect the shape functions, $\phi_i, i = 1, \ldots 4$, as:

$$\Phi = \{\phi_1, \phi_2, \phi_3, \phi_4\} \tag{4}$$

Here, $\Phi$ is the list and its elements $\phi_i$ are encased within curly braces.

The requirement of *exactly reproducing an arbitrary linear field* dictates:

$$\phi_1 + \phi_2 + \phi_3 + \phi_4 = 1 \tag{5}$$

$$x_1\ \phi_1 + x_2\ \phi_2 + x_3\ \phi_3 + x_4\ \phi_4 = x \tag{6}$$

$$y_1\ \phi_1 + y_2\ \phi_2 + y_3\ \phi_3 + y_4\ \phi_4 = y \tag{7}$$

Without any loss in generality, let us assume that $\phi_2$ be given. Then we can obtain $\phi_1, \phi_3,$ and $\phi_4$ by solving equation (5) through equation (7). For example, $\phi_1$ can be solved in the form:

$$\phi_i = \frac{\text{numerator}_i}{\text{denominator}}, \quad i = 1, 3, 4; \qquad \text{denominator} = \det \begin{bmatrix} 1 & x_1 & y_1 \\ 1 & x_3 & y_3 \\ 1 & x_4 & y_4 \end{bmatrix} \tag{8}$$

The nonvanishing determinant mandates that nodes $1, 3$ and $4$ cannot be colinear for $\phi_1, \phi_3$ and $\phi_4$ to be solvable in terms of $\phi_2$. The selection of the side node to be the second one meets such a criterion. In the formulation, $\phi_1, \phi_3$ and $\phi_4$ will be obtained in terms of $\phi_2$.

As a clarification of the notations used here, it may be observed that a matrix is encased within square brackets [...], *vide* equation (8).

*3.1. Orientation of the element*

In order to keep the algebraic expressions compact, the formulation is demonstrated with a convenient orientation of the element as shown in Figure 5, the original orientation for the generalized case is represented in Figure 4.

The following geometrical transformations are performed to obtain Figure 5 from Figure 4 :

(a) the element is so translated that the second node falls on the origin;

(b) the element is so rotated about the origin that the first and the third nodes fall on the $x-$axis;

(c) the element is so oriented that the vertex, i.e., the fourth node, falls on the positive $y-$region.

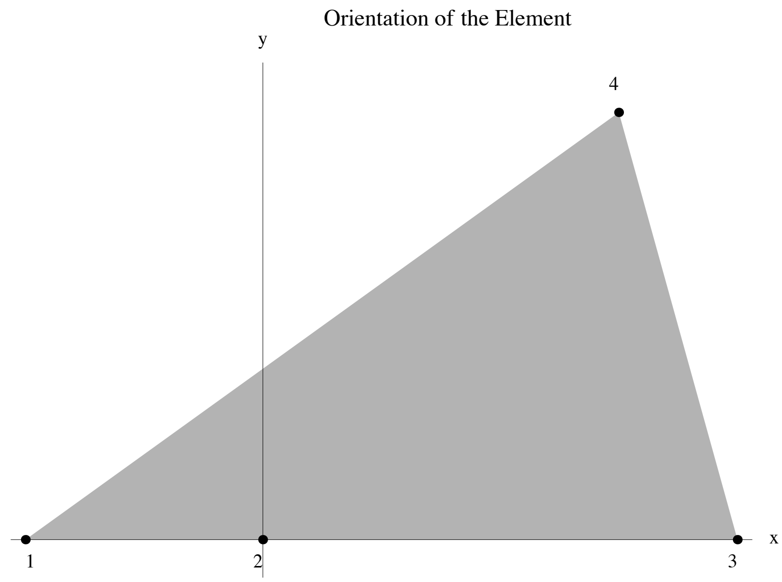


Figure 5: Canonical orientation: side node at the origin and three nodes on $x-$axis

### *3.2. Construction of the shape function associated with the (intermediate) side node*

In equation (8), in order to avoid the vanishing of the denominator determinant, $\phi_2$, which is the shape function associated with the side node, is to be determined first. Subsequently, the other three shape functions are obtained using equations (5) through (7).

The first step is to construct a function, which will be linear between the nodes 1 and 2, and nodes 2 and 3, with a unit value at node 2 as shown in Figure 6.

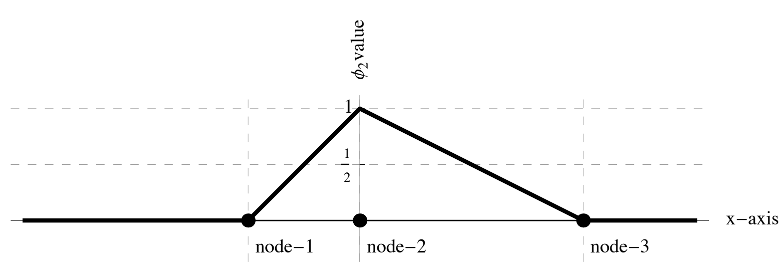


Figure 6: The “hat” function on the $x-$ axis

*3.2.1. The slope discontinuity for the "hat" function*

The discontinuity in the slope at node 2 can be realized in terms of the Heaviside's step function:

$$H(x) = \begin{cases} = 0, & x < 0, \\ = 1, & x > 0; \end{cases} \tag{9}$$

or, equivalently, by selecting the positive branch of the square root function:

$$\sqrt{x^2} = \begin{cases} = -x, & x < 0, \\ = \ \ x, & x > 0; \end{cases} \tag{10}$$

which is identical to the absolute value function:

$$\|x\| = \begin{cases} = -x, & x < 0, \\ = \ \ x, & x > 0; \end{cases} \tag{11}$$

Using equation (9):

$$\sqrt{x^2} = \|x\| = x\,\Big(H(x) - \ H(-x)\Big) \tag{12}$$

*3.2.2. The "hat" function*

Linear combination of $x$ and $\sqrt{x^2}$ are illustrated leading to the "hat" function shown in Figure 6. The procedure is illustrated step by step starting with the graph of the $\sqrt{x^2}$ function. In order to clarify the discontinuities in slopes, an example, *vide* Figure 7(a), with $a = 1, b = 2$ is presented here.

Steps are included as the theoretical formulation is explained. The following numerical data will be used for the element shown in Figure 7(a):

$$a = 1; \quad b = 2; \quad c = \frac{3}{2}; \quad h = \frac{9}{5}; \tag{13}$$

Hence the "hat" function becomes:

$$\hbar(x) = \frac{\mathrm{x} - \sqrt{x^2}}{2\mathrm{a}} - \frac{\sqrt{x^2} + \ \mathrm{x}}{2\mathrm{b}} + 1 \tag{14}$$

hence for the numerical example, the right hand side becomes:

$$\frac{\mathrm{x} - \sqrt{x^2}}{2} - \frac{\sqrt{x^2} + \ \mathrm{x}}{4} + 1 = -\frac{3\sqrt{x^2}}{4} + \frac{3x}{4} + 1 \tag{15}$$

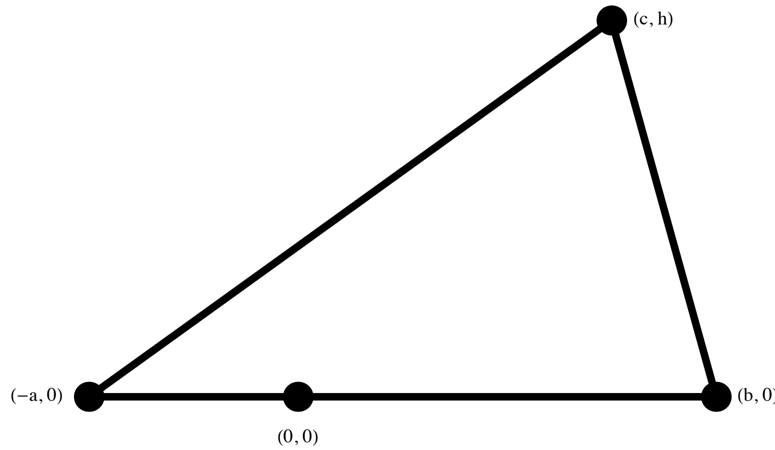


(a) The Element

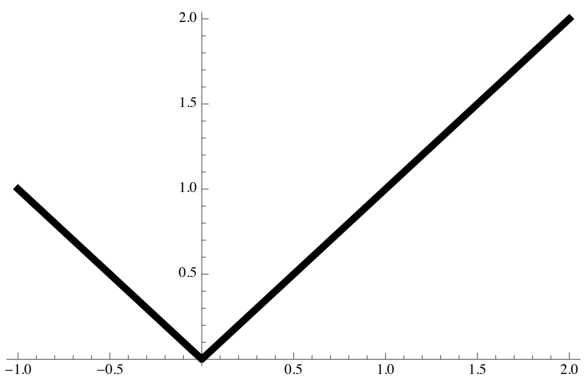


(b) plot of $\sqrt{x^2}$ or $|x|$

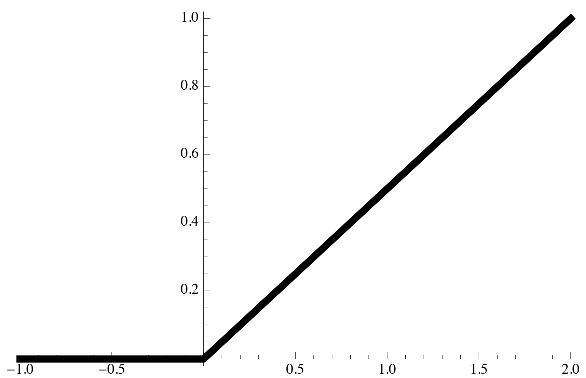


(c) plot of $\frac{x+\sqrt{x^2}}{2b}$

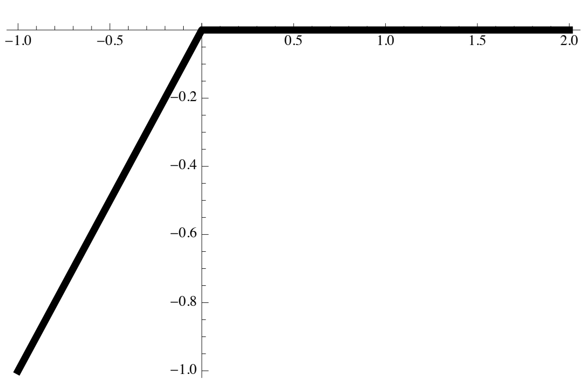


(d) plot of $\frac{x-\sqrt{x^2}}{2a}$

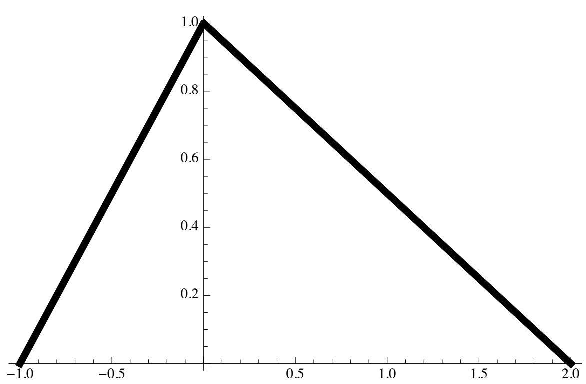


(e) plot of the "hat" function in $x-$axis: $1 + \frac{x-\sqrt{x^2}}{2a} - \frac{x+\sqrt{x^2}}{2a}$

Figure 7: Building up the "hat" function from $\sqrt{x^2}$ or $|x|$

*3.2.3. From a "hat" function to an interpolant*

In order to extend the function $\hbar(x)$ into the triangular region, the equations of the sides $s_{41}, s_{43}$, where $s_{ij}$ is the side joining nodes $i$ and $j$, are written in the following form:

$$\begin{aligned} s_{41} &: 1 - \frac{x}{a_1} - \frac{y}{b_1} = 0 \\ s_{43} &: 1 - \frac{x}{a_3} - \frac{y}{b_3} = 0 \end{aligned} \tag{16}$$

Now equation (16) guarantees that the left hand sides are positive within the triangular finite element and vanish along the sides $s_{41}, s_{43}$. Let the boundary pieces not containing the side node be denoted by $\Gamma$:

$$\Gamma(x, y) = \left\{1 - \frac{x}{a_3} - \frac{y}{b_3} > 0, 1 - \frac{x}{a_1} - \frac{y}{b_1} > 0\right\}, \quad (x, y) \in element \tag{17}$$

$$\text{thus: } \left(\left(1 - \frac{x}{a_3} - \frac{y}{b_3}\right)\left(1 - \frac{x}{a_1} - \frac{y}{b_1}\right)\right) > 0, \quad (x, y) \in element \tag{18}$$

This leads to

$$q(x, y) = \hbar(x)\left(1 - \frac{x}{a_3} - \frac{y}{b_3}\right)\left(1 - \frac{x}{a_1} - \frac{y}{b_1}\right) > 0, \quad (x, y) \in element \tag{19}$$

which vanishes along the sides not containing the intermediate node 2, and has the desired slope discontinuity. In the next step, the unit value of the shape function at node 2 is guaranteed.

Now invoking the Padé form by introducing the appropriate denominator polynomial:

$$\phi_2(x, y) = \frac{q(x, y)}{\left(1 - \frac{x}{a_3}\right)\left(1 - \frac{x}{a_1}\right)} \qquad \text{so that} \quad \phi_2(x, y|_{y=0}) = \hbar(x) \text{ and } \phi_2(0, 0) = 1 \tag{20}$$

In equation (16), in the interception form, the inclined sides of the element can be represented by:

$$a_1 = -a; \qquad a_3 = b; \tag{21}$$

Hence from equation (20):

$$\phi_2(x, y) = \frac{q(x, y)}{\left(1 - \frac{x}{b}\right)\left(1 + \frac{x}{a}\right)} \tag{22}$$

Note that the shape function $\phi_2$ has discontinuities only at those vertices that describe the edge containing the intermediate node.

Using the data from equation (13), equation (22) becomes:

$$\phi_2(x, y) = -\frac{(3\sqrt{x^2} - x - 4)(18x - 25y + 18)(18x + 5y - 36)}{1296(x - 2)(x + 1)} \tag{23}$$

*3.3. Evaluation of all shape functions*

Solutions of equations (5), (6) and (7), using $\phi_2$ from equation (23) yield:

$$\phi_1 = \frac{(18x + 5y - 36)\left(3\sqrt{x^2}(18x - 25y + 18) - 54x^2 + x(25y - 54) + 100y\right)}{1944(x - 2)(x + 1)} \tag{24}$$

$$\phi_3 = \frac{(18x - 25y + 18)\left(3\sqrt{x^2}(18x + 5y - 36) + 54x^2 - x(5y + 108) - 20y\right)}{3888(x - 2)(x + 1)} \tag{25}$$

$$\phi_4 = \frac{5y}{9} \tag{26}$$

The square root expressions, $\sqrt{x^2}$, in equations 24 and 25 could be replaced with the absolute value of $x$ i.e., $\|x\|$.

It should be noted that the denominators of equations 24 and 25 refer to the 'same' adjoint, those polynomials differ only by a multiplicative (scaling) constant. Their singularities are at the end nodes of the base of the triangle (and not at the intermediate node). Thus to obtain unit values of $\phi_1$, and $\phi_3$ the at nodes 1 and 3 respectively, limiting operation according to the L'Hospital rule must be used. The contour plots of the shape functions are showed in Figure 8.

Of course, $\phi_4$ in equation (26), which expresses the shape function for the apex (not connected to the side containing the intermediate node) yields the same answer had there been no side node. This is an important observation to construct shape functions for polygons with an intermediate side node, which is briefly described in this paper with Figure 12.

In equations 24 and 25, the denominator polynomials do not involve $y$ because the orientation in Figure 5 aligns the intermediate node on the $x-$axis. For the original problem, in Figure 4, the appropriate linear transformation for $x$ and $y$ in equations (24) through (26) will yield the shape functions for an arbitrary orientation of the element.

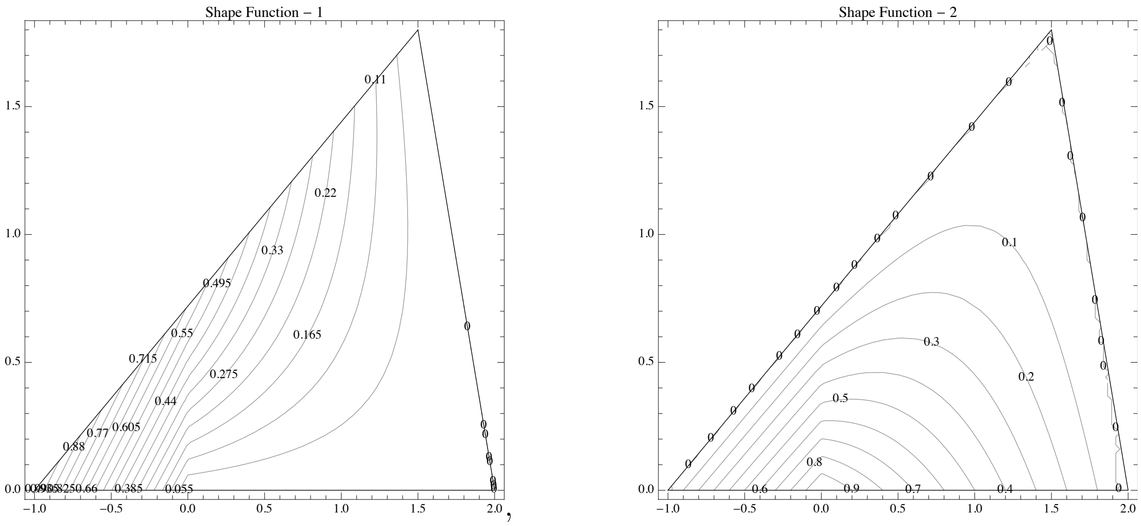


(a) Discontinuities are pronounced

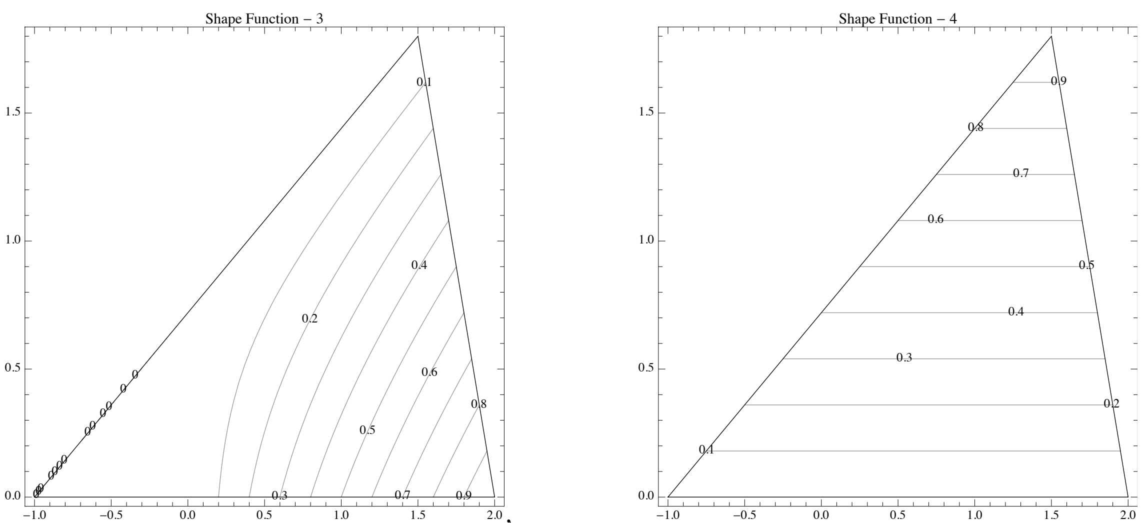


(b) Discontinuities die out away from the side node

Figure 8: Contour plots of shape functions

## 4. Analysis in the light of Wachspress' ***External Intersection Points*** —EIPs

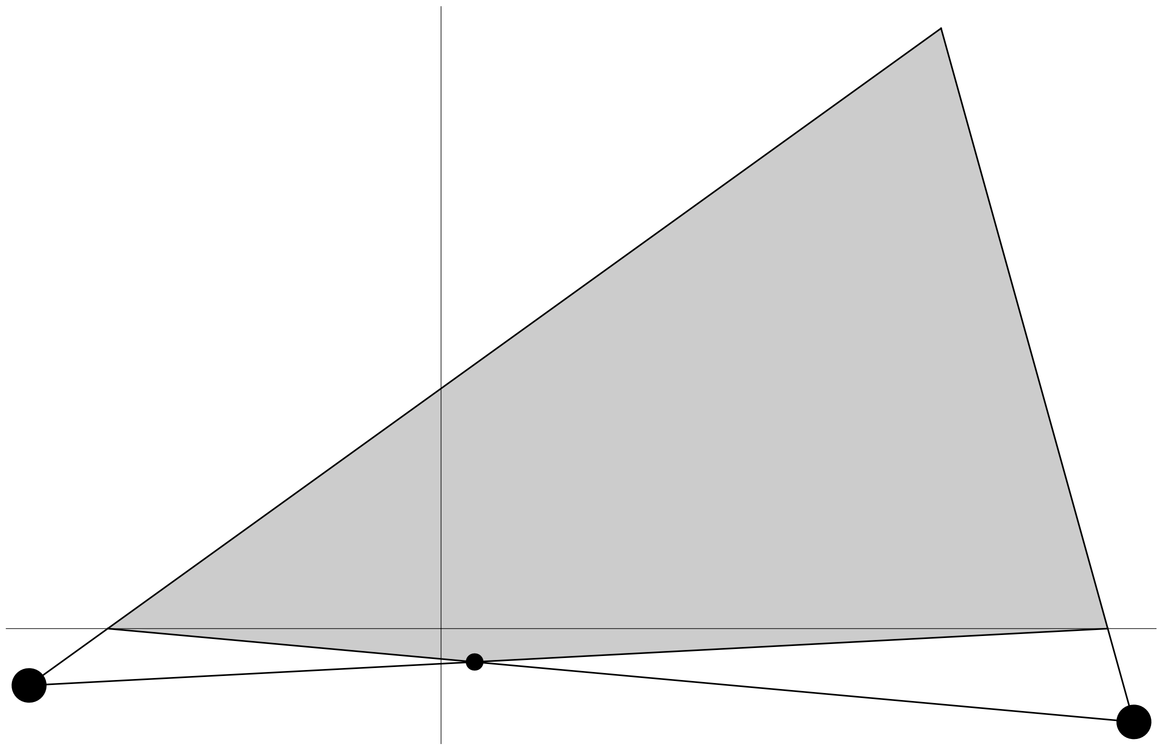

Figure 9: Limiting values of EIPs create singularity at base vertices

The external intersection points (EIPs) are those where the non-adjacent sides intersect outside the convex polygonal region. An important conceptual step in the projective geometric construction of the basis functions is to identify the EIPs, *vide* Wachspress (1971). All shape functions must tend to infinity at the EIPs. The adjoint, the denominator $\nu(x, y)$ in equation (1), is the algebraic curve through all EIPs.

Figure 9 shows the two EIPs necessarily lying on the two sides when the intermediate node on the base is slightly pushed outwards, by a small amount $\epsilon > 0$ to create a convexity. As $\lim \epsilon \to 0$, the EIPs approach the base vertices. Hence it is natural to expect singularities in shape functions associated with the base vertices. This can be verified from equations (24) and (25).

## 5. Comparison with the isoparametric formulation

Using the treatment presented in Dasgupta (2008a), the isoparametric shape functions are obtained as:

$$\phi_1^{(i)} = \frac{1}{36}\sqrt{324x^2 - 180xy + y(25y + 1440)} - \frac{x}{2} - \frac{5y}{12} \tag{27}$$

$$\phi_2^{(i)} = -\frac{1}{24}\sqrt{324x^2 - 180xy + y(25y + 1440)} + \frac{x}{4} + \frac{35y}{72} + 1 \tag{28}$$

$$\phi_3^{(i)} = \frac{1}{72}\sqrt{324x^2 - 180xy + y(25y + 1440)} + \frac{x}{4} - \frac{5y}{8} \tag{29}$$

$$\phi_4^{(i)} = \frac{5y}{9} \tag{30}$$

In the interest of avoiding confusion, a superscript $^{(i)}$ is tagged with the isoparametric shape functions.

The shape function $\phi_2^{(i)}$, which is associated with the side node exactly reproduces the "hat" function:

$$\phi_2^{(i)} = -\frac{1}{24}\sqrt{324x^2 - 180xy + y(25y + 1440)} + \frac{x}{4} + \frac{35y}{72} + 1\Big|_{y=0} = 1 + \frac{x}{4} - \frac{3\sqrt{x^2}}{4} \tag{31}$$

which is identical to equation (15).

A distinguishing feature for the isoparametric shape functions, equations (27) through (29), is that the branch cut of the square root function does not go through the element. This condition was explicitly imposed in the proposed formulation of this paper while solving for the shape functions in the physical $(x, y)$ coordinates.

These isoparametric shape functions, *vide* equations (27) through (29), fail to capture the singularities at nodes 1 and 3, which originate from the projective geometry concepts, shown in equations (27) and (29), compare these with the basis functions of the proposed formulation, *vide* equations (24) and (25).

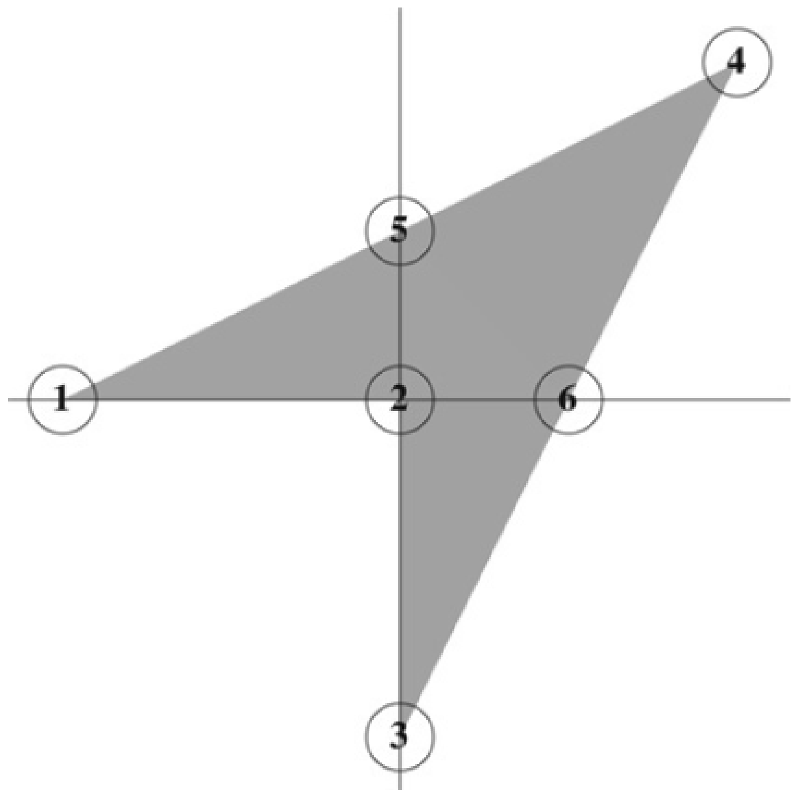


Figure 10: A Convex four node Element

## 6. Square root expressions in the light of concave finite elements

Wachspress established that a two-dimensional concave finite element can be formulated from a three-dimensional projection. Dasgupta and Wachspress (2008b) demonstrated the closed-form construction of shape functions in terms of the $x, y, z$ variables, where, $z$ was equated to $\sqrt{x^2 + y^2}$ when the concavity was set at the origin as shown in Figure 10.

It was not possible to take the limit of the shape functions when the nodes 1, 2 and 3 in Figure 10 become colinear because numerical values of the coordinates were needed to generate the shape functions in $x - y$ variables.

## 7. Conclusions

The square root singularity introduced at the side node causes slope discontinuity in the calculated shape functions. This is demonstrated in Figure 11. Due to the substitution for $y = 0$ in equation (20), the slope discontinuity runs through all along $x = 0$.

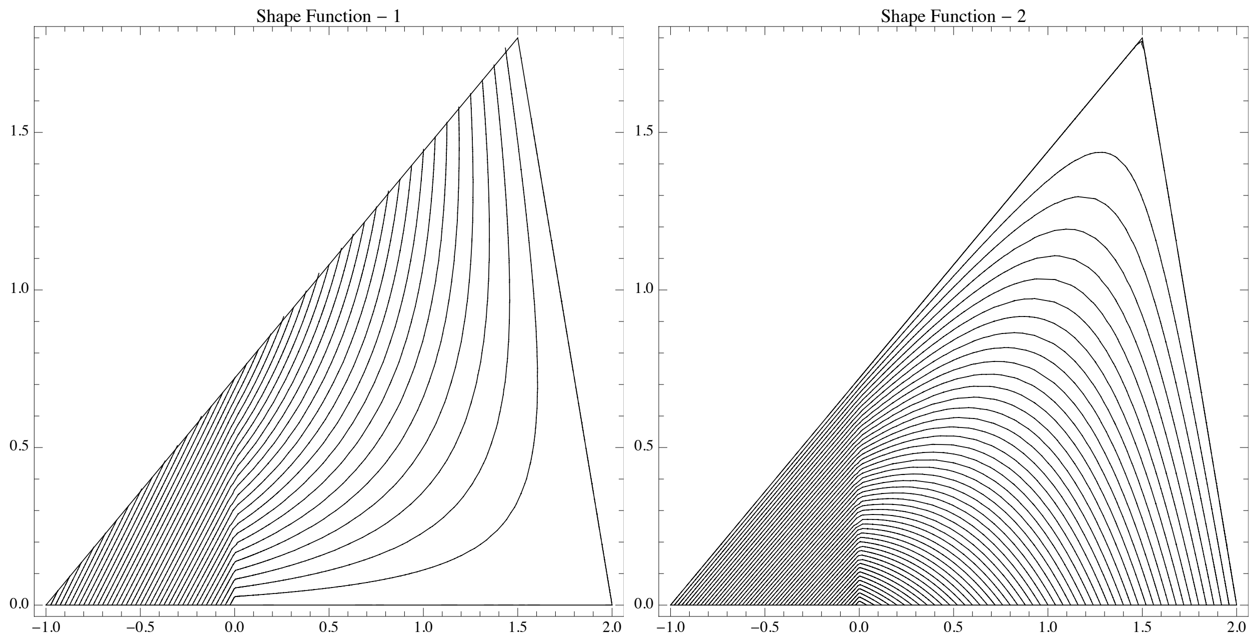


Figure 11: Exaggerated depiction of slope discontinuities of shape functions

Use of computer algebra, specially *Mathematica* in this paper, made it possible to implement the Wachspress method that is based on projective geometry. The ease of formulation for the high accuracy (not contaminated by isoparametric conjecture) finite element is demonstrated in this paper.

*7.1. Extension to a convex polygonal element with a side node*

In this paper, the singularity in the shape function associated with the side node is captured using the square root function. In particular, the shape functions for the triangular element with a side node are computed to examine the procedure to extend the one-dimensional "hat" function into the element region. The same general idea can be applied to convex polygons with a side node, *vide* Figure 12 where an arbitrary convex septagon is shown to contain a side node that lies on the arbitrarily selected side $s_{34}$, which joins nodes 3 and 4, the notation is the same as in equation (16). This extension should be possible because the formulation adheres to the protective geometry concepts, the number of sides is immaterial so long as the geometrical convexity of the element is maintained. This 'generalization concept' was first observed in the ground breaking monograph of Wachspress (1975).

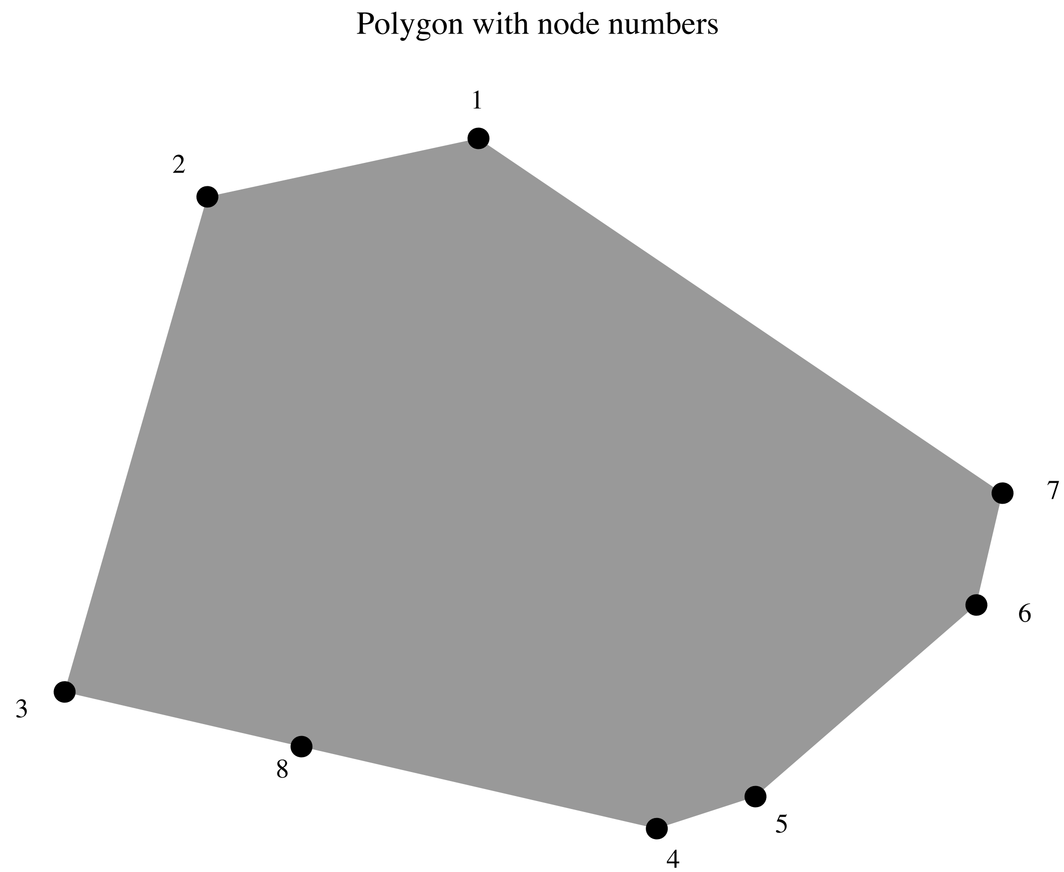


Figure 12: A (seven sided) polygon with a side node

$\Gamma(x, y)$, as in equation (17), be the set of all sides not containing the intermediate node. For the shape functions, $\phi_i(x, y), i = 1 \ldots 8,\ \phi_8(x, y)$ is to be calculated using $\Gamma(x, y)$. The shape functions: $\phi_1(x,y), \phi_2(x,y), \phi_5(x,y), \phi_6(x,y)$ and $\phi_7(x,y)$ will remain the same as those for the septagon without the side node. These five shape functions can be calculated according to Dasgupta (2003b). Using $\phi_8(x,y)$, the two remaining $\phi_3(x,y)$ and $\phi_4(x,y)$ can be determined using linearity conditions described in equation (8).

### *7.2. Comments on symbolic formulation* using the computer algebra software *Mathematica*

Excellent research materials and text books, e.g. Bhatti (2005, 2006), laid out foundation for finite element formulations in terms of closed-form algebraic expressions. These publications have encouraged researchers to carry out 'experiments' with formulations that posed challenges when `Fortran` was the only available tool.

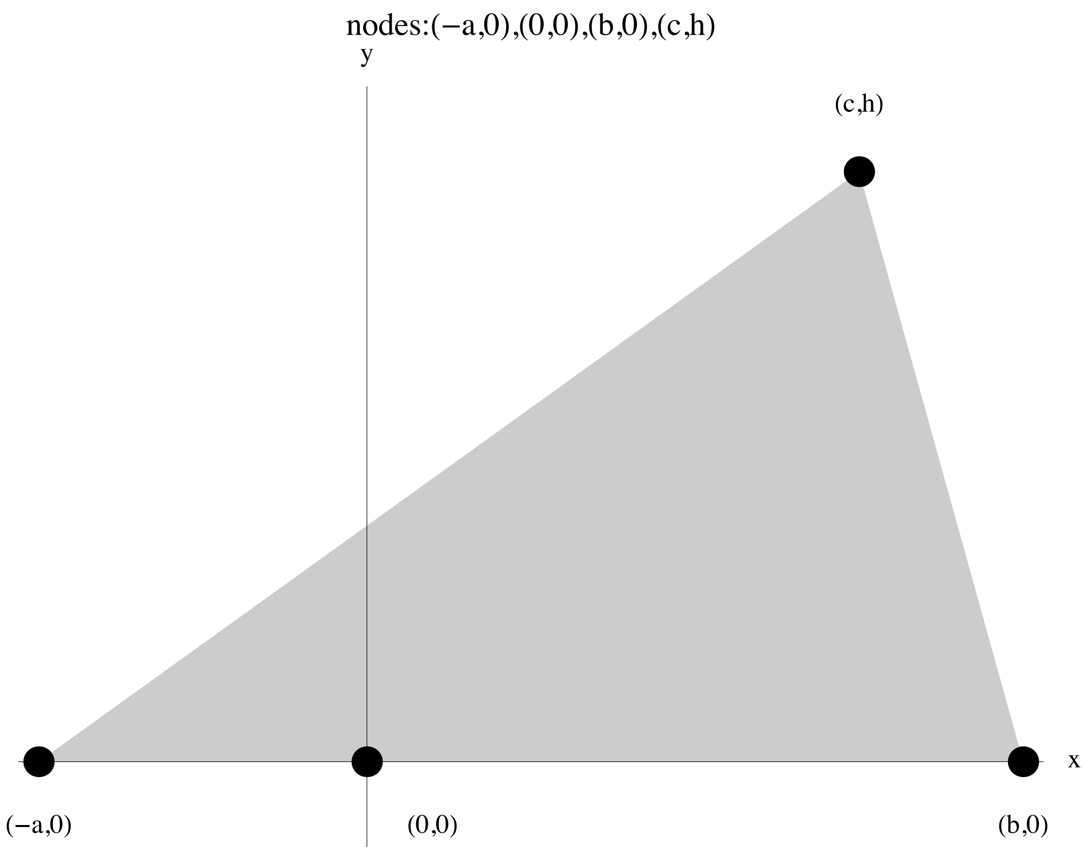


Figure 13: Nodes in terms of algebraic variables

For the triangle with a side node the following closed form shape functions were obtained from *Mathematica* $\TeX$, where $\Big(x * \operatorname{sgn}(x)\Big)$ is identical to $\sqrt{x^2}$ or $\|x\|$:

$$\text{nodes: } (-a,0),(0,0),(b,0),(c,h) \tag{32}$$

yielded:

$$\begin{aligned}\phi_1(x,y) = &\left(\frac{(b(h-y)+cy-hx)}{2ah^2(a+b)(a+x)(b-x)}\right)* \\ &\Bigg(\bigg(\Big(x \operatorname{sgn}(x)\Big)(a+b)(h(a+x)-y(a+c)\bigg) + y(a+c)(2ab-ax+bx)+ \\ &hx(-(a+b))(a+x))\Bigg)\end{aligned} \tag{33}$$

$$\phi_2(x,y) = \frac{\bigg(\Big(x \operatorname{sgn}(x)\Big)(a+b)+a(x-2b)-bx\bigg)(h(a+x)-y(a+c))(b(y-h)-cy+hx)}{2abh^2(a+x)(b-x)} \tag{34}$$

$$\begin{aligned}\phi_3(x,y) = &\left(\frac{h(a+x)-y(a+c)}{2bh^2(a+b)(a+x)(b-x)}\right)* \\ &\Bigg(\Big(x \operatorname{sgn}(x)\Big)(a+b)(b(h-y)+cy-hx)+ \\ &y(b-c)(2ab-ax+bx)+hx(a+b)(b-x)\Bigg)\end{aligned} \tag{35}$$

$$\phi_4(x,y) = \frac{y}{h} \tag{36}$$

These expressions can be easily translated into `Fortran`, `C` and `C`$^{++}$ codes.

## References


G. A. Baker and P. Graves-Morris. Padé approximants. *Encyclopedia of Mathematics and Applications*, 1981.

S. N. Bernstein. Dmonstration du théoréme de weierstrass fondée sur la calcul des probabilités. *Comm. Math. Soc. Kharkov*, 13, 1913.

M. Asghar Bhatti. *Fundamental Finite Element Analysis and Applications: with Mathematica and Matlab Computations*. John Wiley, 2005. ISBN-13: 978-0471648086.

M. Asghar Bhatti. *Advanced Topics in Finite Element Analysis of Structures: With Mathematica and MATLAB Computations*. John Wiley, 2006. ISBN: 978-0-471-64807-9.

R. Courant. Variational methods for the solution of problems of equilibrium and vibration. *Bulletin of the American Mathematical Society*, 49:1–29, 1943.

H.S.M. Coxeter. *Projective Geometry*. Springer, New York, NY, 2000. First 1964 edition published by Blaisdell Publishing Company, Second 1974 edition published by Toronto University Press.

G. Dasgupta. Integration within polygonal finite elements. *Journal of Aerospace Engineering, ASCE*, 16(1):9–18, January 2003a.

G. Dasgupta. Interpolants within convex polygons: Wachspress' shape functions. *Journal of Aerospace Engineering, ASCE*, 16(1):1–8, January 2003b.

G. Dasgupta. Closed-form isoparametric shape functions of four-node convex finite elements. *Journal of Aerospace Engineering, ASCE*, 21:10 – 18, January 2008a.

G. Dasgupta. Stiffness matrices of isoparametric four-node finite elements by exact analytical integration. *Journal of Aerospace Engineering, ASCE*, 21(2):45 – 50, April 2008b.

G. Dasgupta and E.L. Wachspress. The adjoint for an algebraic finite element. *Computers and Mathematics with Applications*, 55(9):1988–1997, May 2008a.

G. Dasgupta and E.L. Wachspress. Basis functions for concave polygons. *Computers and Mathematics with Applications*, 56(2):459–468, July 2008b.

Carl de Boor. *B-splines*. Springer-Verlag, 1978. Series: Applied Mathematical Sciences, Vol. 27.

J. D. Foley, A. Van Dam, S. K. Feiner, and J. F. Hughes. *Computer Graphics Principles and Practice*. Addison-Wesley, 2nd edition, 1996.

P. Fritzson. *Principles of Object-Oriented Modeling and Simulation*. John Wiley & Sons, 2004. Modelica 2.1. Book, 800 pages. Accepted for publication (jointly) by IEEE Press and Wiley, February 2003; ISBN 0471471631.

P. Fritzson. *MathCode*. MathCore Engineering AB, 2011.

William G.Gray and Martinus Th. Van Genuchten. Economical alternatives to gaussian quadrature over isoparametric quadrilaterals. *International Journal of Numerical Methods in Engineering*, 12, 1978. Short Communication.

Jean-Louis Gout. *Elements finis polygonaux de Wachspress*. PhD thesis, L'université de Pau et des pays de l'adour, June 6 1980. Thèse de doctorat d'état es-sciences mathématiques, le grade de Doctoeur-es-sciences.

Charles Hermite. Sur la formule d'interpolation de lagrange. *Journal für die reine und angewandte mathematik*, 84:84–49, 1877.

Shi-Pin Ho and Yen-Liang Yeh. The use of 2d enriched elements with bubble functions for finite element analysis. *Computers & Structures*, 84:2081 — 2091, 2006.

Gabor L. Hornyak, Joydeep Dutta, H.F. Tibbals, and Anil Rao. *Introduction to Nanoscience*. CRC Press, 2008. ISBN-10: 1420048058, ISBN-13: 978-1420048056.

B. M. Irons. Quadrature rules for brick based finite elements. *International Journal of Numerical Methods in Engineering*, 3, April/June 1971.

B. M. Irons and A. Razzaque. *Experience with the patch test for convergence of finite elements method*. Academic Press, New York, 1972.

Elisabeth Anna Malsch, John Jeffy Lin, and Gautam Dasgupta. Smooth two-dimensional interpolations: A recipe for all polygons. *Journal of Graphics, GPU, & Game Tools*, 10(2):27—39, 2005. DOI:10.1080/2151237X.2005.10129192.

C. D . Mote. Global-local finite element. *International Journal for Numerical Methods in Engineering*, 3, 1971.

E. Mousavi, E. Grinspun, and N. Sukumar. Higher-order extended finite elements with harmonic enrichment functions for complex crack problems. *International Journal for Numerical Methods in Engineering*, December 2010. DOI: 10.1002/nme.309.

V. C. Mow and R. Huiskes. *Basic Orthopaedic Biomechanics and Mechano-Biology.* Lippincott Williams & Wilkins, 3rd. edition, 2005. SBN 0-7817-3933-0, BioMedical Engineering OnLine 2005, 4:28 doi:10.1186/1475-925X-4-28.

W. Ritz. Über eine neue methode zur lösung gewisser variationalprobleme der mathematischen physik. *Journal Reine Angew. Math.*, 135, 1908.

Suzanne M. Shontz and Stephen A. Vavasis. Analysis of and workarounds for element reversal for a nite element-based algorithm for warping triangular and tetrahedral meshes. *BIT Numerical Mathematics*, 50:863 – 884, 2010.

N. Sukumar. Geometric design, computer graphics, and fem, 2007. November 4 – 8.

N. Sukumar and E. A. Malsch. Recent advances in the construction of polygonal finite element interpolants. *Archives of Computational Methods in Engineering*, 13(1):129—163, 2006. DOI: 10.1007/BF02905933.

I. C. Taig. Structural analysis by the matrix displacement method. Report S017, English Electric Aviation Report, England, 1961.

E. L. Wachspress. *A Rational Basis for Function Approximation*, volume 228 of *Lecture Notes in Mathematics*. Springer Verlag, 1971.

E. L. Wachspress. *A Rational Finite Element Basis.* Academic Press, 1975.

P. Yiu. The uses of homogeneous barycentric coordinates in plane euclidean geometry. *International Journal of Mathematical Education in Science and Technology*, 31, 2000.